J Mol Model (2012) 18:4199–4207
DOI 10.1007/s00894-012-1421-4

ORIGINAL PAPER

Quantum chemical investigations aimed at modeling highly efficient zinc porphyrin dye sensitized solar cells

Ahmad Irfan · Naz Hina · Abdullah G. Al-Sehemi · Abdullah M. Asiri

Received: 19 January 2012 / Accepted: 29 March 2012 / Published online: 4 May 2012
© Springer-Verlag 2012

Abstract Zinc tetraphenylporphyrin (ZnTPP) was modified by a push-pull strategy and then density functional theory (DFT) and time-dependent DFT (TD-DFT) calculations were performed for the resulting derivatives. The smallest HOMO–LUMO energy gaps were found in ZnTPP-6 and ZnTPP-7, which had nitro substituents and a conjugated chain, while the largest was observed for ZnTPP-5. The energy gaps of all of the systems designed in this work were smaller than that of ZnTPP. Clear intramolecular charge transfer was observed from donor to acceptor in ZnTPP-6 and ZnTPP-7, which had nitro groups at positions R8, R9, and R10, as well as in ZnTPP-3 and ZnTPP-4, which had cyano groups at those positions. The narrow band gaps (compared to that of ZnTPP) of these designed systems, where the LUMO is above the conduction band of TiO_2 and the HOMO is below the redox couple, indicate that they are efficient sensitizers. The B bands of these newly designed derivatives, except for ZnTPP-5, are redshifted compared with the B band of ZnTPP.

Keywords Dye-sensitized solar cell · Porphyrin · Density functional theory · Frontier molecular orbitals · Absorption

A. Irfan (✉) · A. G. Al-Sehemi
Chemistry Department, Faculty of Science,
King Khalid University,
Abha, Saudi Arabia
e-mail: irfaahmad@gmail.com

N. Hina
Institute of Chemistry, University of the Punjab,
Lahore 54590, Pakistan

A. M. Asiri
Chemistry Department, Faculty of Science,
King Abdulaziz University,
P.O. Box 80203,
Jeddah 21589, Saudi Arabia

A. M. Asiri
Center of Excellence for Advanced Materials Research,
King Abdulaziz University,
P.O. Box 80203,
Jeddah 21589, Saudi Arabia

Introduction

Among all of the renewable energy technologies developed so far, the nanocrystalline dye-sensitized solar cell (DSSC) system, a kind of photovoltaic device presented by O'Regan and Gratzel in 1991, has generated a lot of interest due to its potential application to low-cost solar-based electricity generation [1]. Dye sensitizers based on organometallic complexes, especially ruthenium polypyridyl complexes such as N3 and black dye (as presented by Gratzel et al.), give the best performance of all dye sensitizers, with efficiencies of greater than 11 % [2]. However, Ru is an expensive and rare metal, and it is not environmentally friendly, so metal-free dyes have been the focus of much research. Campbell and coworkers have developed a range of colored dyes for use in DSSCs [3, 4]. High-performance DSSCs have also attracted attention, as they exhibit low viscosities and high conductivities, resulting in large diffusion coefficients [5, 6].

The electronic structure, absorption properties, and electron transfer dynamics at the interface between dyes and nanocrystalline materials have been studied by various groups [2, 7–10]. Both porphyrins (Ph) and phthalocyanines (Pc) are classes of dyes that are considered attractive alternatives to expensive and polluting pyridyl-based Ru complexes, the former because of their similarity to natural photosynthetic molecules, and the latter because of their photochemical and thermal

stabilities [11]. The unique optical properties of metalloporphyrins are useful for many technological applications [12–14]. It has been demonstrated that metalloporphyrins can potentially be utilized as light-harvesting dyes in solar cells, and zinc porphyrin derivatives are particularly effective in this context [15, 16].

The main aim of research in this field is to prepare dyes that are very efficient when used in a DSSC, and which fulfill the following basic requirements. Firstly, the sensitizing dyes must firmly bond to the photocatalyst plane to ensure very rapid electron insertion into the conduction band of TiO_2. Secondly, the lowest unoccupied molecular orbital (LUMO) of the dye must be sufficiently higher in energy than the conduction band of TiO_2 for efficient charge insertion, and the highest occupied molecular orbital (HOMO) of the dye must be lower in energy than the hole-transport material (HTM) for efficient regeneration of the oxidized dye [17, 18]. Most of the supramolecular chemistry of these macrocycles has focused on porphyrins due to their well-developed chemistry. In addition to their chemical and photophysical similarities to the hemes and chlorophylls, porphyrins are ideal molecules for assembling photonic systems. In general, porphyrins have very strong absorption bands at around 400–430 nm (the Soret band) and several Q bands between 500 and 650 nm. Their electronic spectra depend on the exocyclic modifications and coordinated metal ion present in the porphyrins, which are well explained by the Gouterman four-orbital model [19].

The other porphyrinoids also show strong absorption, which is generally more towards the red region compared to the porphyrins [20]. The geometric characteristics of metalloporphyrins are very useful for many applications, including photodynamic therapy light harvesting, nonlinear absorption, and optical storage. The UV/visible absorption areas of porphyrins are of great value when these molecules are processed for use as sensitizers in solar cells. In a very interesting set of studies of porphyrin arrays, Bocian and coworkers proposed that the order of the porphyrin frontier orbitals plays a crucial role in determining the rates of electronic communication [21, 22]. Tetraphenylporphyrin (TPP) is synthetic heterocyclic compound that resembles naturally occurring porphyrins.

Therefore, in the investigation described in the present paper, the well-known planar molecule zinc tetraphenylporphyrin (ZnTPP) molecule was modified in an attempt to enhance its sensitizing efficiency, thus generating a series of ZnTPP derivatives (ZnTPP-1 to ZnTPP-7). The effects of varying the conjugated linkers (in terms of length and type) in the molecule were explored (Fig. 1). In ZnTPP1, a COOH group was added at R1 of ZnTPP and cyanide groups at R7, R12, and R16. In ZnTPP-2, COOH groups were added at R2, R7, R12, and R17. In ZnTPP-3, a four-carbon conjugated chain was added at R1 with an anchoring COOH

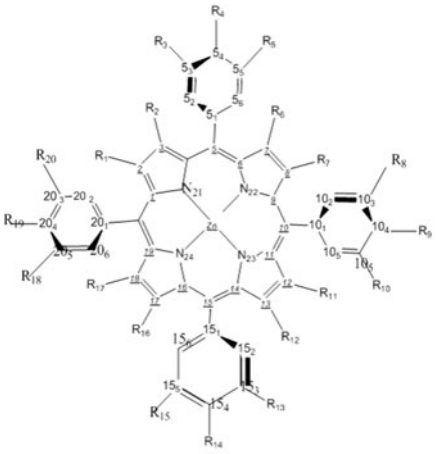

	Substituent =R
1	R 1= —COOH and R7,R12 R16 = —C≡N
2	R2,R7,R12,R17= —COOH
3	R1= , R8,R9,R10= —C≡N, R18,R19.R20=
4	R1= , R8,R9,R10= —C≡N, R18,R19,R20= , R12=
5	R1= , R8,R9,R10= —F, R18,R19.R20=
6	R1= , R8,R9,R10= —NO2, R18,R19.R20=
7	R1= , R8,R9,R10= —NO2, R18,R19.R20= , R12=

Fig. 1 ZnTPP and the derivatives of ZnTPP investigated in the present study

group at the end, while cyanide groups were inserted at R8, R9, and R10 and donor methyl groups were included at R18, R19, and R20. In ZnTPP-4, conjugated chains with an anchoring COOH group at the end were inserted at R1 and R11, while cyanide gropus were added at R8, R9, and R10, and methyl groups at R18, R19, and R20. In ZnTPP-5, a conjugated chain was included at R1, fluorines at R8, R9, and R10, and methyl groups at R18, R19, and R20. In ZnTPP-6, a conjugated chain was added at R1, nitro groups at R8, R9, and R10, and methyl groups at R18, R19, and R20. Finally, in ZnTPP-7, conjugated chains were included at R1 and R11, nitro groups at R8, R9, and R10, and methyl groups at R18, R19, and R20.

We carried out DFT and TDDFT calculations to optimize the geometries of these sensitizers, evaluated their electronic properties and absorption spectra, and

then compared our theoretical results to experimental data. This approach was implemented to enhance our understanding of the effect of the presence of particular substituents in a porphyrin on its electronic and optical properties (i.e., we explored the structure–property relationship for these sensitizers).

This theoretical study should therefore aid in the design of novel, more efficient sensitizers. The development of enhanced sensitizers is crucial to the optimization of DSSCs, and depends on a quantitative understanding of dye sensitizers. This means that theoretical investigations of the physical properties of dye sensitizers are very important, as they allow us to explore how sensitizer performance is related to sensitizer structure and properties, ultimately leading to the design and production of novel dye sensitizers with improved performance.

Computational details

All of the calculations were carried out with the G09 software package [23]. Density functional theory (DFT) is well known to be suitable for calculating the chemical and structural properties of species, such as organic semiconductors, optoelectronics, and conventional inorganic semiconductors [24–31]. Electronic properties of carbon nanotubes and graphene nanoribbons have been investigated using the Heyd −Scuseria−Ernzerhof (HSE) screened exchange hybrid and the hybrid meta-generalized functional of Tao, Perdew, Staroverov, and Scuseria (TPSSh). Moreover, Wu et al. investigated composites consisting of a finite single-walled carbon nanotube (SWCNT) and impurities (two lanthanide atoms) using a plane-wave density functional theory method [32, 33]. Because carbon nanotubes and nanoribbons can contain

Table 1 Calculated bond lengths (in Å) in ZnTPP and its derivatives, calculated at the B3LYP/6-31 G* (LANL2DZ) level of theory

	ZnTPP	ZnTPP-1	ZnTPP-2	ZnTPP-3	ZnTPP-4	ZnTPP-5	ZnTPP-6	ZnTPP-7
C1–C2	1.446	1.458	1.430	1.471	1.472	1.471	1.472	1.472
C2–C3	1.345	1.368	1.368	1.377	1.378	1.377	1.377	1.377
C3–C4	1.449	1.438	1.457	1.430	1.430	1.430	1.430	1.430
C4–C5	1.402	1.410	1.412	1.417	1.417	1.416	1.416	1.417
C5–C6	1.404	1.412	1.415	1.406	1.406	1.408	1.406	1.406
C6–C7	1.449	1.434	1.439	1.446	1.445	1.447	1.447	1.447
C7–C8	1.358	1.373	1.369	1.361	1.360	1.362	1.361	1.361
C8–C9	1.441	1.460	1.459	1.449	1.448	1.448	1.449	1.449
C9–C10	1.403	1.410	1.416	1.412	1.410	1.411	1.412	1.400
C10–C11	1.407	1.411	1.415	1.412	1.416	1.411	1.412	1.416
C11–C12	1.442	1.436	1.459	1.448	1.433	1.448	1.448	1.433
C12–C13	1.349	1.371	1.369	1.362	1.376	1.362	1.362	1.377
C13–C14	1.442	1.463	1.438	1.446	1.472	1.447	1.447	1.472
C14–C15	1.407	1.412	1.412	1.400	1.412	1.410	1.409	1.412
C15–C16	1.403	1.412	1.410	1.413	1.416	1.412	1.413	1.416
C16–C17	1.441	1.462	1.438	1.445	1.446	1.446	1.446	1.447
C17–C18	1.359	1.371	1.367	1.361	1.361	1.362	1.362	1.361
C18–C19	1.442	1.436	1.450	1.448	1.447	1.448	1.448	1.447
C19–C20	1.405	1.414	1.410	1.414	1.414	1.414	1.414	1.414
C1–N21	1.373	1.375	1.374	1.378	1.376	1.377	1.376	1.377
C4–N21	1.375	1.375	1.377	1.375	1.375	1.376	1.376	1.375
C6–N22	1.368	1.376	1.374	1.378	1.378	1.377	1.377	1.378
C9–N22	1.378	1.373	1.375	1.372	1.373	1.375	1.372	1.373
C14–N23	1.379	1.373	1.373	1.378	1.378	1.376	1.372	1.373
C11–N23	1.379	1.376	1.375	1.372	1.373	1.374	1.377	1.378
C19–N24	1.378	1.376	1.377	1.376	1.376	1.375	1.375	1.376
C16–N24	1.371	1.373	1.375	1.375	1.374	1.376	1.375	1.374
N21–Zn	2.063	2.079	2.069	2.083	2.080	2.084	2.083	2.090
N22–Zn	2.063	2.082	2.074	2.068	2.062	2.065	2.068	2.061
N23–Zn	2.075	2.066	2.073	2.070	2.093	2.078	2.070	2.094
N24–Zn	2.071	2.070	2.079	2.059	2.040	2.059	2.059	2.049

hundreds of carbon atoms, the B3LYP functional should not be used in attempts to reproduce experimental data for such molecules. In recent studies performed by us, the B3LYP functional was used to investigate the electronic properties of tris(8-hydroxyquinolinato) aluminum derivatives, triphenylamine-based sensitizers, and tin phthalocyanine derivatives [34–37], and applying the B3LYP functional yielded results that agreed reasonably well with the corresponding experimental data. Thus, in the present study, we used B3LYP to shed light on the electronic properties of Zn porphyrin derivatives. The structures investigated in the present study were optimized in the ground state (S_0) at the B3LYP/6-31G* (LANL2DZ) level of theory. Absorption spectra were calculated using time-dependent density functional theory (TD-DFT) at the B3LYP/6-31G* (LANL2DZ) level of theory, which has been shown to be an accurate method for zinc porphyrins [8, 9]. The LANL2DZ basis set was applied, which was found to be precise for metal-containing systems [38–42].

Results and discussion

Geometries

The computed geometrical parameters for ZnTPP are shown in Table 1, and are in good agreement with other theoretical as well as experimental data [42–47]. We now discuss the bond lengths of the investigated systems in comparison to those of ZnTPP. In ZnTPP-1, the bond lengths of C2–C3, C7–C8, C12–C13, C13–C14, and C16–C17 are longer than those of ZnTPP by 0.023, 0.015, 0.022, 0.021, and 0.021 Å, respectively. This is because, at R1 in ZnTPP-1, a carboxylic group is present at the β position, which attracts charge, causing the charge density at C2 to decrease and thus the length of the C2–C3 bond to increase. As there are cyanide groups at R7, R12, and R16 that also attract charge, all four of the C–C bonds that have β substituents increase in length.

In ZnTPP-2, the lengths of the bonds C2–C3, C8–C9, C12–C13, and C18–C19 are 0.023, 0.018, 0.02, and

Table 2 Calculated bond angles (in °) for ZnTPP and its derivatives, calculated at the B3LYP/6-31 G* (LANL2DZ) level of theory

Angles	ZnTPP	ZnTPP-1	ZnTPP-2	ZnTPP-3	ZnTPP-4	ZnTPP-5	ZnTPP-6	ZnTPP-7
C1–C2–C3	107.49	106.71	107.65	105.53	105.49	105.56	105.53	105.47
C6–C7–C8	106.75	107.34	107.60	107.14	107.18	107.13	107.13	107.17
C11–C12–C13	107.23	107.42	107.44	107.08	108.33	107.11	107.08	108.31
C16–C17–C18	106.70	106.85	107.61	107.08	107.16	107.11	107.09	107.17
C1–N21–C4	106.70	107.73	107.98	107.66	107.57	107.73	107.67	107.57
C6–N22–C9	106.38	108.00	107.98	107.27	107.26	107.27	107.27	107.25
C11–N23–C14	106.10	108.21	107.87	107.24	107.61	107.24	107.24	107.60
C16–N24–C19	106.46	108.26	107.91	107.33	107.41	107.38	107.33	107.41
N21–Zn–N22	89.07	90.24	90.13	90.73	90.41	90.73	90.72	90.42
N22–Zn–N23	88.59	90.13	89.20	89.63	90.38	89.68	89.66	90.39
N23–Zn–N24	88.28	89.72	90.75	89.92	89.57	89.93	89.88	89.55
N24–Zn–N21	88.72	89.90	89.96	89.74	89.64	89.69	89.76	89.65
C4–C5–C6	125.30	124.10	124.98	125.61	125.37	125.66	125.60	125.40
$C5_2$ –$C5_3$–$C5_4$	120.27	120.18	120.11	120.18	120.19	120.18	120.18	120.18
$C5_3$–$C5_4$ –$C5_5$	119.67	119.68	119.68	119.65	119.64	119.61	119.65	119.64
$C5_4$–$C5_5$–$C5_6$	120.15	120.18	120.24	120.18–	120.18	120.19	120.18	120.19
C9–C10–C11	125.50	124.97	124.33	125.80	126.04	125.50	125.88	126.16
$C10_2$–$C10_3$–$C10_4$	120.33	120.10	120.15	120.31	120.32	121.27	121.51	121.51
$C10_3$–$C10_4$–$C10_5$	119.57	119.85	119.76	118.44	118.42	118.51	117.34	117.33
$C10_4$–$C10_5$–$C10_6$	120.04	120.12	120.15	120.31	120.33	121.28	121.51	121.52
C14–C15–C16	125.26	124.78	125.19	125.21	125.45	125.28	125.18	125.48
$C15_2$ –$C15_3$–$C15_4$	119.74	120.07	120.17	120.18	120.17	120.18	120.18	120.17
$C15_3$–$C15_4$ –$C15_5$	120.58	119.99	119.65	119.63	119.69	119.61	119.63	119.69
$C15_4$–$C15_5$–$C15_6$	119.72	120.06	120.13	120.19	120.13	120.19	120.189	120.13
C19–C20–C1	125.41	124.73	125.34	125.54	125.36	125.58	125.57	125.43
$C20_2$–$C20_3$–$C20_4$	120.27	120.22	120.09	119.73	119.75	119.74	119.73	119.76
$C20_3$–$C20_4$–$C20_5$	119.49	119.72	119.69	119.40	119.38	119.38	119.40	119.38
$C20_4$–$C20_5$–$C20_6$	120.08	120.10	120.23	119.38	119.39	119.37	119.39	119.38

0.018 Å longer than those of ZnTPP, respectively. Because carboxylic acid is present at the β position and is a strongly electron-withdrawing group, it attracts charge from its neighboring carbons, decreasing the electron density at the carbon atom and increasing the bond length.

In ZnTPP-3, the C1–C2 bond length is increased by 0.025 Å compared to that of ZnTPP, C2–C3 is increased by 0.032 Å, and N21–Zn is increased by 0.02 Å because a conjugated chain with an anchoring carboxylic group at the end is present at R1. This group attracts charge, resulting in longer C–C bonds. It has also been observed that C–C bonds close to cyanide groups are relatively long.

In ZnTPP-4, C1–C2, C2–C3, C12–C13, C13–C14, N21–Zn, and N23–Zn are increased by 0.026, 0.033, 0.027, 0.03, 0.017, and 0.018 Å compared to ZnTPP, respectively, because conjugated chains are present at R1 and R11, and these chains have a COOH group at the end that attracts electronic charge. This decreases the electron density at its neighboring atoms, leading to increased C–C bond lengths.

Table 3 HOMO energies (E_{HOMO}), LUMO energies (E_{LUMO}), and HOMO–LUMO energy gaps (E_{gap}), all in eV, of ZnTPP and its derivatives, calculated at the B3LYP/6-31 G* (LANL2DZ) level of theory

System	E_{HOMO}	E_{LUMO}	E_{gap}
ZnTPP	−5.13	−2.39	2.74
ZnTPP-1	−5.69	−3.16	2.53
ZnTPP-2	−5.23	−2.69	2.54
ZnTPP-3	−5.46	−2.99	2.47
ZnTPP-4	−5.55	−3.14	2.41
ZnTPP-5	−5.16	−2.61	2.55
ZnTPP-6	−5.46	−3.20	2.26
ZnTPP-7	−5.54	−3.27	2.27

In ZnTPP-5, the C1–C2 bond length is increased by 0.025 Å, C2–C3 by 0.032 Å, and N21–Zn by 0.021 Å compared to ZnTPP, because at a conjugated chain with an anchoring carboxylic group at the end is present at R1, which draws charge towards it and thus increases neighboring C–C bond lengths. N24–Zn is decreased by 0.012 Å because methyl groups are present at R18, R19, and R20, and the methyl group is an

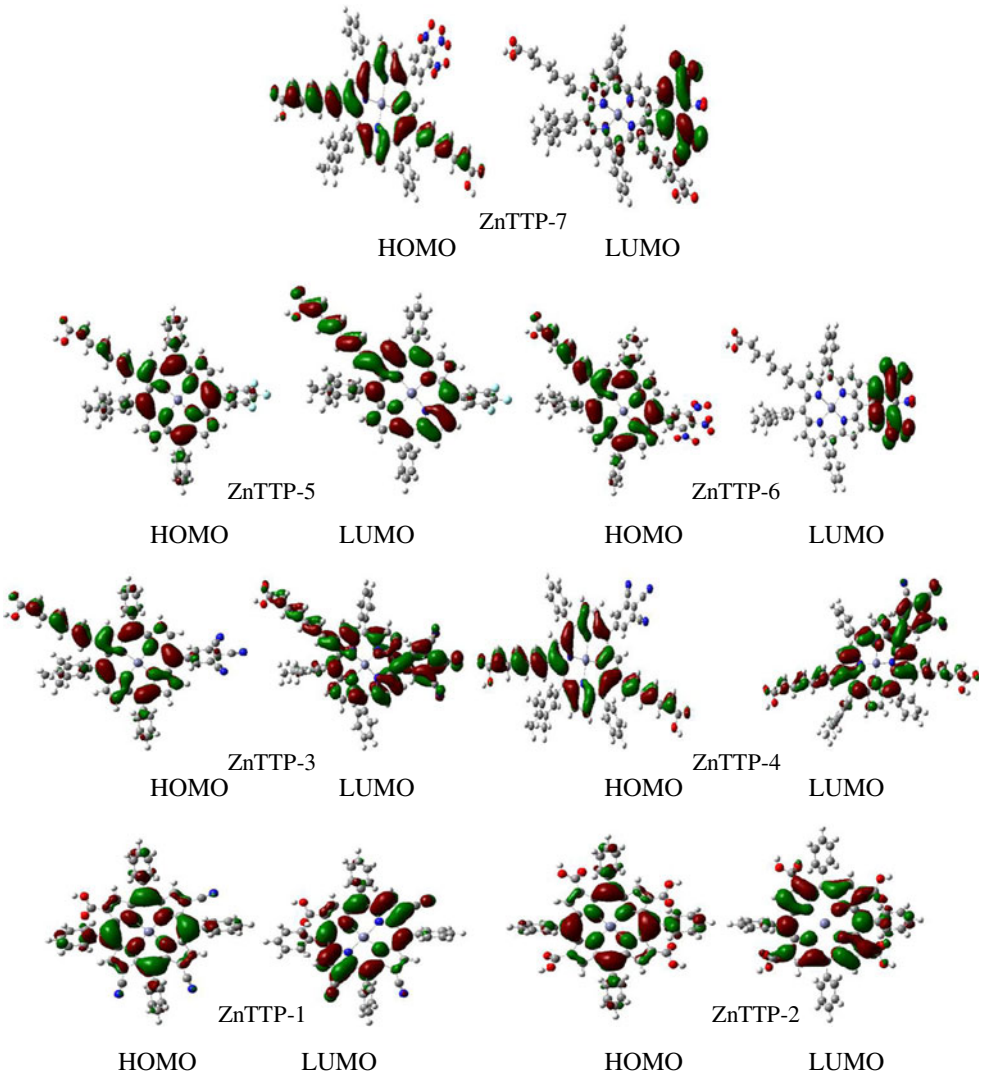

Fig. 2 The HOMOs and LUMOs of the systems investigated in the present study

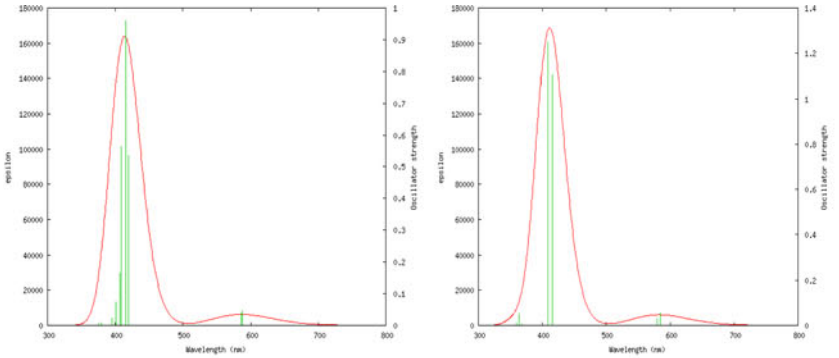

ZnTPP-1 ZnTPP-2

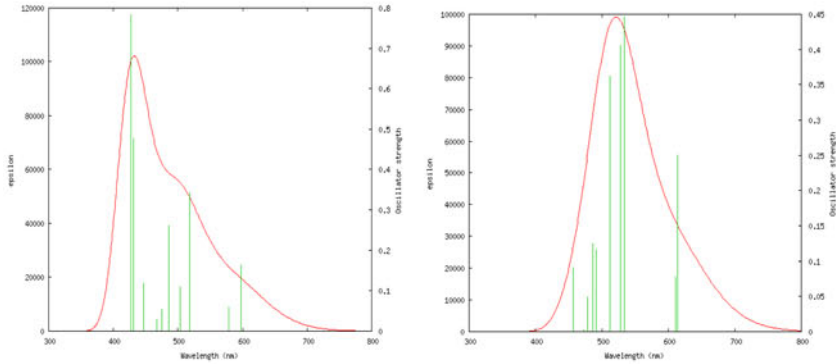

ZnTPP-3 ZnTPP-4

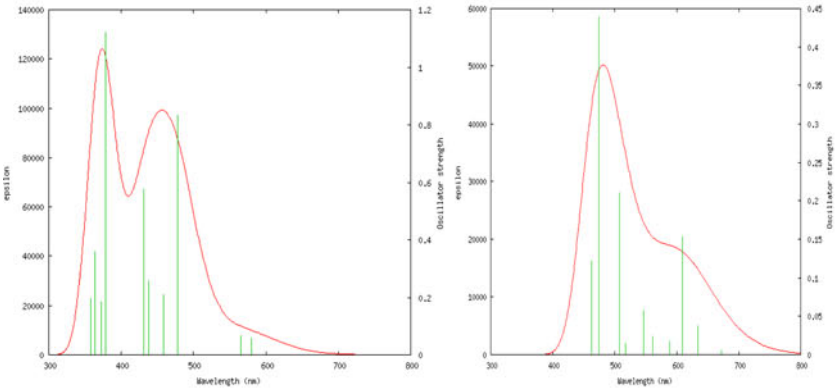

ZnTPP-5 ZnTPP-6

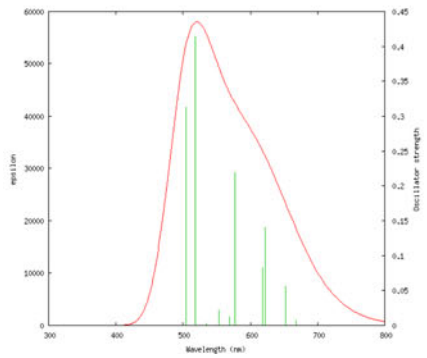

ZnTPP 7

Fig. 3 The absorption spectra of ZnTPP and its derivatives, calculated at the B3LYP/6-31 G* (LANL2DZ) level of theory

electron donor. Thus, N24 in ZnTPP-5 exhibits greater electron density than N24 in ZnTPP, and this extra charge density attracts the nearest atom, decreasing the corresponding bond length.

In ZnTTP-6, increases of 0.026, 0.032, and 0.013 Å are observed for the bonds C1–C2, C2–C3, and C12–C13, respectively. N21–Zn is increased by 0.02 Å because a conjugated chain is present at R1 (see above for an explanation of the effect of this chain). N24–Zn is decreased by 0.012 Å because methyl groups are present at R18, R19, and R20 (again, see above for the explanation). In ZnTPP-7, C1–C2 is increased by 0.026 Å, C2–C3 by 0.032 Å, C12–C13 by 0.023 Å, and C13–C14 by 0.03 Å, while N24–Zn is decreased by 0.022 Å, all for the same reasons as mentioned above.

In ZnTPP-1, the angles C1–N21–C4, C11–N23–C14, and C16–N24–C19 are increased by 1.62°, 2.11°, and 1.8°, respectively, when compared with ZnTPP (see Table 2). In ZnTPP-2, the bond angles are similar to those observed in ZnTPP. In ZnTPP-3, the C1–C2–C3 bond angle is decreased by 1.96°. In ZnTPP-4, the C1–C2–C3 bond angle is decreased by 1.93°, while the C11–C12–C13 bond angle is increased by 1.1°. In ZnTPP-5, the C1–C2–C3 bond angle is decreased by 1.93°; in ZnTPP-6, the C1–C2–C3 bond angle is decreased by 1.96°; in ZnTPP-7, the C1–C2–C3 bond angle is decreased by 2.02°, and the C11–C12–C13 bond angle is increased by 1.08° compared with ZnTPP.

Electronic properties

To design efficient porphyrin-based sensitizers intended for use in DSSCs, the candidate molecule must have certain characteristics. First, it should have a narrow band gap, with the LUMO (lowest unoccupied molecular orbital) of the dye lying just above the conduction band of TiO_2. It is well known that if the LUMO of dye is above the conduction band of TiO_2, electron transfer from the dye to TiO_2 becomes favorable. Second, the HOMO (highest occupied molecular orbital) of the dye should be below the redox couple (the electrolyte in which the dye is regenerated; generally an iodide/triiodide mixture is used as the redox couple in a DSSC). Third, the HOMO should be located on the donor moiety and the LUMO on the acceptor moiety to achieve the most efficient charge transfer. The size of the HOMO–LUMO gap (the potential energy difference between the HOMO and LUMO) can be used as an index of kinetic stability [48]. Kaur et al. investigated the relationship between the size of the HOMO–LUMO gap and photooxidative resistance [49]. The implications of predicting the HOMO–LUMO gaps of π-conjugated systems on the design of new materials with specified properties have been discussed and analyzed [50]. The HOMO–LUMO gap is basically the energy that must be fed to the molecule to kick it from the ground state to an excited state. A large gap means that high-energy radiation, such as UV, is required to do this. A small gap means that lower-energy radiation, such as green or even red light, is needed [51]. The link between the HOMO–LUMO gap and the electronic properties of the molecule have also been investigated [51]. A smaller energy gap leads to a redshift in the absorption spectrum [52].

The distribution patterns of the HOMOs and LUMOs of the systems studied in this work are shown in Fig. 2. In ZnTPP-1, the HOMO is distributed in the center of the ring. Carboxylic acid and cyanide groups are both electron-withdrawing in nature, but they do not appear to draw the electronic charge towards them in this case. This may be due to the metal inside the porphyrin ring, which is a Lewis acid that also attracts the charge. On the other hand, the charge density for the LUMO is distributed not only at the center of the ring, but also toward the cyanide groups at positions 7 and 16.

The HOMO in ZnTPP-2 is delocalized at the center of the ring, while some of the charge density is distributed on all of the phenyl rings. The delocalization of the charge at the center may again due to the central metal, which is a Lewis acid and thus attracts the charge. For the LUMO, the charge density is distributed at the center of the ring as well as on the phenyl rings at positions C10 and C20.

In ZnTPP-3, the HOMO is distributed at the center of the ring and also on the conjugated chain, because the anchoring carboxylic group attracts charge. The methyl groups attached to C18, C19, and C20 donate electronic charge to the porphyrin ring. For the LUMO, the charge distribution is focused on the porphyrin ring, the conjugated chain, and the phenyl rings containing cyanide groups at C8, C9, and C10, as they are strongly electron-withdrawing and thus attract the electronic charge. None of the other phenyl rings are included in the charge distribution.

In ZnTPP-4, the HOMO is delocalized on the porphyrin ring and the conjugated chains on both sides. For the LUMO, the charge is distributed on the porphyrin ring, the conjugated chains, and the phenyl rings containing cyanide groups at C8, C9, and C10, for the reason described above. In ZnTPP-5, the HOMO is delocalized on the porphyrin ring, towards the conjugated carbon chain, and slightly on the phenyl rings. The LUMO charge distribution occurs on the conjugated chain and on the ring. In ZnTTP-6, the

Table 4 Positions of the B and Q bands (in nm) in the absorption spectra of ZnTPP[a] and its derivatives, as calculated at the B3LYP/6-31 G* (LANL2DZ) level of theory

System	B band	Q band
ZnTPP	382	540
ZnTPP-1	415	587
ZnTPP-2	418	584
ZnTPP-3	427	530
ZnTPP-4	428	–
ZnTPP-5	378	478
ZnTPP-6	474	608
ZnTPP-7	518	621

[a]Experimentally, the B and Q bands of ZnTPP are found at 423 nm and 556 nm, respectively [9]

charge density of the HOMO is delocalized on the porphyrin ring and towards the conjugated chains. The charge density for the LUMO is attracted by the strongly electron-withdrawing nitro groups; all of the charge distribution occurs on the phenyl ring containing nitro groups. Proper intramolecular charge transfer is observed in this case. In ZnTPP-7, the electronic charge density is located at the center and on the two conjugated chains. For the LUMO, the highest charge density is observed on the phenyl ring containing the nitro groups, as they are strongly electron-withdrawing. Intramolecular charge transfer is clearly apparent in this case. In ZnTPP-6 and ZnTPP-7, the HOMO is localized on the donor moiety and LUMO is on the acceptor moiety. In ZnTPP-3 and ZnTPP-4, the HOMO is localized at the donor site and the LUMO is on the acceptor moiety, leading to efficient charge transfer in these materials.

The HOMO and LUMO energies of the bare $(TiO_2)_{38}$ cluster (a nanocrystalline model) are −7.23 and −4.1 eV, respectively, resulting in a HOMO–LUMO gap of 3.13 eV [17]. An energy gap of >0.2 eV between the LUMO of the dye and the conduction band of TiO_2 is usually necessary for effective electron injection [18]. Indeed, the LUMO energies of previously designed dyes are above the conduction band of TiO_2. On other hand, the HOMO of the redox couple (I^-/I_3^-) is −4.8 eV [47]. As we mentioned above, the LUMO of the dye must be above the conduction band of TiO_2 and the HOMO most be below the redox couple to achieve an efficient sensitizer. Thus, a narrow band gap leads to an efficient sensitizer. From Table 3, it is apparent that the HOMOs of the systems investigated here are below the redox couple. Moreover, the HOMO–LUMO gaps of the derivatives are all smaller than that of ZnTPP, which indicates that these materials would be efficient sensitizers. The computed HOMO energy, LUMO energy, and HOMO–LUMO energy gap for ZnTPP are −5.13, −2.14, and 2.74, respectively, which are in good agreement with the calculated data of Ma et al. [42]. The smallest HOMO–LUMO energy gaps are found for ZnTPP-6 and ZnTPP-7, which also show the best intramolecular charge-transfer properties. The trends for the HOMO energies, LUMO energies, and HOMO–LUMO energy gaps are: ZnTPP> ZnTPP-5> ZnTPP-2 >ZnTPP-3=ZnTPP-6 > ZnTPP-7=ZnTPP-4 > ZnTPP-1; ZnTPP>ZnTPP-5 > ZnTPP-2>ZnTPP-3 > ZnTPP-4>ZnTPP-1 >ZnTPP-6>ZnTPP-7; and ZnTPP> ZnTPP-5 > ZnTPP-2 >ZnTPP-1>ZnTPP-3 >ZnTPP-4 > ZnTPP-7>ZnTPP-6, respectively (see Table 3).

Optical properties

When the B band of ZnTPP is compared with those of its derivatives, the B bands of ZnTPP-1, ZnTPP-2, ZnTPP-3, ZnTPP-4, ZnTPP-6, and ZnTPP-7 appear to be redshifted and that of ZnTPP-5 is blueshifted (see Fig. 3 and Table 4). The Q bandsof ZnTPP-1, ZnTPP-2, ZnTPP-6, and ZnTPP-7 are redshifted while those of ZnTPP-3 are ZnTPP-5 blue-shifted compared to the Q band of ZnTPP. ZnTPP has its B band at 382 nm and Q band at 540 nm. For ZnTPP-1, the B band is at 415 nm and the Q band at 587 nm. For ZnTPP-2, the B band occurs at 418 nm and the Q band at 584 nm. For ZnTPP-3, the B band is at 427 nm and the Q band at 530 nm. For ZnTPP-4, the B band is found at 428 nm and no Q band is observed. For ZnTPP-5, the B band can be seen at 378 nm and the Q band at 478 nm. For ZnTPP-6, the B band is at 474 nm and the Q band at 608 nm. Finally, for ZnTPP-7, the B band appears at 518 nm and the Q band at 621 nm.

Conclusions

The ground-state geometries of ZnTPP and seven derivatives (ZnTPP-1 to ZnTPP-7) of it were computed at the B3LYP/6-31 G* (LANL2DZ) level of theory. Time-dependent DFT was applied to investigate their absorption spectra. Major changes in bond lengths were noted in the derivatives containing a conjugated chain with a COOH anchoring group and nitro or cyano groups as substituents. The smallest HOMO–LUMO energy gaps were observed for ZnTPP-6 and ZnTPP-7, which contained nitro group substituents and conjugated chains. The largest HOMO–LUMO energy gap was observed for ZnTPP-5. Clear intramolecular charge transfer was observed in ZnTPP-3, ZnTPP-4, ZnTPP-6, and ZnTPP-7. Because the LUMOs of the derivatives are all above the conduction band of TiO_2 and their HOMOs are below the redox couple, and they have narrow band gaps compared to ZnTPP, these derivatives should be efficient sensitizers. They should be highly efficient due to easy electron transfer. When the B band of ZnTPP was compared with those of itsderivatives, it is clear that the B bands of ZnTPP-1, ZnTPP-2, ZnTPP-3, ZnTPP-4, ZnTPP-6, and ZnTPP-7 are redshifted while that of ZnTPP-5 is blueshifted. Finally, the Q bands of ZnTPP-1, ZnTPP-2, ZnTPP-6, and ZnTPP-7are redshifted while ZnTPP-3 and ZnTPP-5 are blueshifted compared to the Q band of ZnTPP.

Acknowledgments We are thankful to King Khalid University for its support and for providing the facilities needed to carry out the research work.

References

1. O'Regan B, Gratzel M (1991) Nature 353:737–740
2. Nazeeruddin MK, Angelis FD, Fantacci S, Selloni A, Viscardi G, Liska P, Ito S, Takeru B, Gratzel M (2005) J Am Chem Soc 127:16835–16847

3. Wang Q, Campbell WM, Bonfantani EE, Jolley KW, Officer DL, Walsh PJ, Gordon K, Humphry-Baker R, Nazeeruddin MK, Gratzel M (2005) J Phys Chem B 109:15397–15409
4. Go Sun Solutions (2012) Website. http://gosunsolutions.com/home/content/view/46/2/
5. Bai Y, Cao YM, Zhang J, Wang MK, Li RZ, Wang P, Zakeeruddin SM, Gratzel M (2008) Nature Mat 7:626–630
6. Gao F, Wang Y, Shi D, Zhang J, Wang MK, Jing XY, Humphary-Baker R, Wang P, Zakeeruddin SM, Gratzel M (2008) J Am Chem Soc 130:10720–10728
7. Tsai HH, Simpson MC (2002) Chem Phys Lett 353:111–118
8. Walsh PJ, Gordon KC, Officer DL, Campbell WM (2006) J Mol Struct (THEOCHEM) 759:17–24
9. Cleland DM, Gordon KC, Officer DL, Wagner P, Walsh PJ (2009) Spectrochim Acta Part A 74:931–935
10. Duncan WR, Prezhdo OV (2007) Ann Rev Phys Chem 58:143–184
11. Claessens CG, Hahn U, Torres T (2008) Chem Rec 8:75–97
12. Milgrom LR (1997) The colours of life: an introduction to the chemistry of porphyrins and related compounds. Oxford University Press, Oxford
13. Choi M-S, Yamazaki T, Yamazaki I, Aida T (2004) Angew Chem Int Ed 43:150–158
14. Dong ZC, Guo XL, Wakayama Y, Hou JG (2006) Surf Rev Lett 13:143–147
15. Campbell WM, Jolley KW, Wagner P, Wagner K, Walsh PJ, Gordon KC, Schmidt-Mende L, Nazeeruddin MK, Wang Q, Graetzel M, Officer DL (2007) J Phys Chem C 111:11760–11762
16. Xiang N, Zhou W, Jiang S, Deng L, Liu Y, Tan Z, Zhao B, Shen P, Tan S (2011) Sol Energy Mater Sol Cells 95:1174–1181
17. Angelis FD, Fntacci S, Selloni A (2008) Nanotechnology 19:424002
18. Ito S, Zakeeruddin SM, Humphry-Baker R, Liska P, Charvet R, Comte P, Nazeeruddin MK, Péchy P, Takata M, Miura H, Uchida S, Grätzel M (2006) Adv Mater 18:1202–1205
19. Gouterman M (1978) In: Dolphin D (ed) The porphyrins, vol 3. Academic, New York, pp 1–153
20. Smith KM (1972) Porphyrins and metalloporphyrins. Elsevier, Amsterdam
21. Strachan JP, Gentemann S, Seth J, Kalsbeck WA, Lindsey JS, Holten D, Bocian DF (1997) J Am Chem Soc 119:11191–11201
22. Yang SI, Seth J, Balasubramanian T, Kim D, Lindsey JS, Holten D, Bocian DF (1999) J Am Chem Soc 121:4008–4018
23. Frisch MJ et al (2009) Gaussian 09, revision A.1. Gaussian Inc., Wallingford
24. Bhattacharjee CR, Das G, Purkayastha DD, Kanoo P, Mondal P (2011) J Coord Chem 64:2746–2760
25. Tsai FC, Chang CC, Liu CL, Chen WC, Jenekhe SA (2005) Macromolecules 38:1958–1966
26. Cao H, Ma J, Zhang G, Jiang Y (2005) Macromolecules 38:1123–1130
27. Hutchison GR, Ratner MA, Marks TJ (2005) J Phys Chem B 109:3126–3138
28. Hutchison GR, Ratner MA, Marks TJ (2005) J Am Chem Soc 127:2339–2350
29. Salzner U, Lagowski JB, Pickup PG, Poirier RA (1998) Synth Met 96:177–189
30. Salzner U (2001) Synth Met 119:215–216
31. Delley B (2000) J Chem Phys 113:7756–7764
32. Wu J, Hagelberg F (2011) J Phys Chem C 115:4571–4577
33. Barone V, Hod O, Peralta JE, Scuseria GE (2011) Acc Chem Res 44:269–279
34. Irfan A, Cui R, Zhang J, Nadeem M (2010) Aust J Chem 63:1–7
35. Irfan A, Nadeem M, Athar M, Kanwal F, Zhang J (2011) Comput Theor Chem 968:8–11
36. Irfan A, Al-Sehemi AG, Asiri AM (2012) J Mol Model. doi:10.1007/s00894-012-1372-9
37. Irfan A, Al-Sehemi AG, Asiri AM, Nadeem M, Alamry KA (2011) Comput Theor Chem 977:9–12
38. Wan L, Zhang YX, Qi DD, Jiang JH (2010) J Mol Graphics Modell 28:842–851
39. Liu ZQ, Chen ZX, Jin BB, Zhang XX (2011) Vib Spectr 56:210–218
40. Li L, Tang Q, Li H, Yang X, Hu W, Song Y, Shuai Z, Xu W, Liu Y, Zhu D (2007) Adv Mater 19:2613–2617
41. Irfan A, Zhang J, Chang Y (2009) Chem Phys Lett 483:143–146
42. Ma R, Guo P, Yang L, Guo L, Zeng Q, Liu G, Zhang X (2010) J Mol Struct (THEOCHEM) 942:131–136
43. Byrn MP, Curtis CJ, Goldberg I, Hsiou Y, Khan SI, Sawin PA, Tendick SK, Strouse CE (1991) J Am Chem Soc 113:6549–6557
44. Nemykin VN, Basu P (2001) Virtual molecular orbital description program (VMOdes). Department of Chemistry, Duquesne University, Pittsburgh
45. Scheidt WR, Kastner ME, Hatano K (1978) Inorg Chem 17:706–710
46. Golder AJ, Povey DC (1990) Acta Crystallogr C 46:1210–1212
47. Balanay MP, Kim DH (2008) Phys Chem Chem Phys 10:5121–5127
48. Aihara JI (1999) J Phys Chem A 103:7487–7495
49. Kaur I, Jia W, Kopreski RP, Selvarasah S, Dokmeci MR, Pramanik C, McGruer NE, Miller GP (2008) J Am Chem Soc 130:16274–16286
50. De Oliveira MA, Duarte HA, Pernaut J-M, De Almeida WB (2000) J Phys Chem A 104:8256–8262
51. do Couto PC, Guedes RC, Cabral BJC (2004) Braz J Phys 34:42–47
52. Irfan A, Cui RH, Zhang JP, Hao LZ (2009) Chem Phys 364:39–45